





Speed-adjustable atomic beam of metastable helium for precision measurementJ.-J. Chen (陈娇娇)¹, Y. R. Sun (孙羽)^{1,2,*}, J.-L. Wen (温金录)¹ and S.-M. Hu (胡水明)^{1,2}¹*Hefei National Laboratory for Physical Sciences at Microscale, iChem Center, University of Science and Technology of China, Hefei 230026, China*²*CAS Center for Excellence in Quantum Information and Quantum Physics, University of Science and Technology of China, Hefei 230026, China*

(Received 13 March 2020; accepted 26 March 2020; published 11 May 2020)

A bright beam of metastable helium atoms is useful in various studies. Laser spectroscopy of helium in an atomic beam can provide a determination of the fine-structure constant and the nuclear charge radius, towards a test of quantum electrodynamics (QED). In these measurements, it is necessary to control not only the internal quantum state but also the translation motion of the helium atom. Here we present a setup producing an intense and speed-adjustable continuous beam of helium atoms. By using a combination of laser cooling, focusing, and deflection, helium atoms are prepared at the single quantum state of 2^3S_1 ($m = 0$), with a very narrow distribution of the longitudinal speed ($\delta v_z < \pm 4.5$ m/s). At the same time, we obtain a flux of 1.8×10^{13} (atoms/s)/sr with a fractional fluctuation below 0.02%. The atomic-beam quality was investigated by laser spectroscopy, indicating a considerable improvement over those used in previous helium precision-spectroscopy measurements.

DOI: [10.1103/PhysRevA.101.053824](https://doi.org/10.1103/PhysRevA.101.053824)**I. INTRODUCTION**

An intense, stable, and collimated atomic-beam source is necessary in many studies, such as improving the experimental accuracy in precision spectroscopy [1,2], reducing the relative uncertainty of atomic clocks [3], rapid preparation of atomic Bose-Einstein condensates [4], and forming high-intensity continuous atomic lasers [5]. The study of collisions between low-speed neutral atoms and molecules is also a field that is developing rapidly [6–8]. Research in this direction is thought to open the door to cold chemistry [9]. Low-energy collision experiments require precise control of the speed of atoms and molecules, especially the relative speed of collision beams, which is corresponding to the reaction energy, a key parameter for studying collision experiments [10–12].

In these studies, preparation of as many atoms as possible in a single quantum state is required. Moreover, control of the translation motion of atoms in the beam is also critical to improve the accuracy in relevant measurements [1,2]. However, it is a considerable experimental challenge to control the speed of the atomic beam without a significant loss in the beam intensity. A time-of-flight method was applied to select hydrogen atoms with different velocities in the atomic beam [13], but the beam flux dramatically decreased when slow atoms were selected. For atoms in which laser cooling can be implemented, it is possible to decelerate atoms with lasers, such as using a Zeeman slower. Without losing efficiency, difficulties still exist when using a counterpropagating laser beam to slow and separate atoms from the background beam. However, sufficient flux is always needed in atomic-beam-based precision measurement.

Precision spectroscopy of helium has received extensive attention as an effective method to test quantum electrodynamics (QED). The accuracy of the calculated fine-structure splitting of the 2^3P energy level of atomic helium can currently reach the order of kilohertz [14–19], which is aimed at an independent measure of the fine-structure constant. The calculated $2S - 2P$ transition frequency of atomic helium is expected to break through the accuracy of 10 kHz in the future [20]. The comparison between the calculated and experimental frequencies also allows for a determination of the charge radius of the helium nucleus with an accuracy of 10^{-3} , which could be directly compared to the results obtained by the μHe^+ system [20]. Such a comparison is analogous to that of the $e\text{H}-\mu\text{H}$ system [2,21,22] and verifies our current understanding of lepton interaction, which is of great significance in fundamental physics.

Here we introduce a system of a speed-adjustable, high-brightness, and stable helium atomic beam. By using a combination of laser cooling, deflection, and Zeeman slower, we realized the control of the speed of the metastable (2^3S_1) helium atoms. The speed of the atomic beam is adjustable from 50 to 450 m/s, with a narrow distribution of less than ± 4.5 m/s, corresponding to a temperature of 10 mK. At the same time, the transverse divergence half angle of the atomic beam is < 2.1 mrad, and the brightness reaches 1.8×10^{13} (atoms/s)/sr. The beam will allow a significant improvement in the precision spectroscopy of helium.

II. EXPERIMENT

The schematic of the speed-adjustable atomic helium beam system is shown in Fig. 1. Helium gas is first precooled by liquid nitrogen, and then a radio-frequency discharge excites the helium atoms from the ground state 1^1S_0 to the 2^1S_0 and 2^3S_1 states. Compared to our previous setup [23], a new

*Corresponding author: robert@ustc.edu.cn

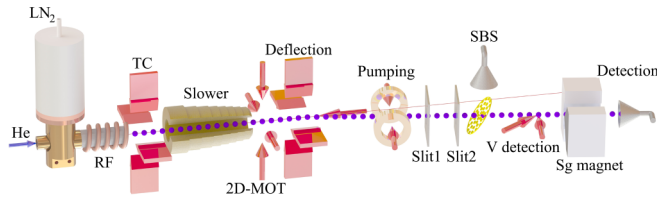


FIG. 1. Schematic of the experimental setup. LN₂: liquid nitrogen; RF: radio-frequency discharge; TC: transverse cooling; SBS: stable beam system; Sg magnet: Stern-Gerlach magnet.

vacuum system equipped with larger turbo pumps was employed. The background pressure decreased to the 10^{-7} Pa level in the source chamber. Consequently, the collision loss is reduced and the flux of the metastable helium atoms at the 2^3S_1 state increases. A transverse cooling device was installed inside the vacuum chamber instead of outside, which collimates the metastable atoms using the 1083 nm $2^3S - 2^3P$ transition. Metastable atoms are then focused by a two-dimensional magneto-optical trap (2D-MOT) and pass through a Zeeman slower. Atoms are decelerated from the original speed of 820 m/s to as low as 50 m/s. The final speed can be adjusted by changing the frequency of the cooling laser and the magnetic field of the Zeeman slower. Subsequently, a second 2D-MOT further compresses metastable helium atoms, which are heated due to the Zeeman slower. A second transverse cooling laser deflects the collimated metastable atoms from the previous beam direction by an angle of 5.7° . Therefore, the 2^3S_1 metastable atoms are separated from background beam containing ground-state atoms, 2^1S_0 state atoms, UV photons, and other particles [24–26]. A pump laser excites atoms in the 2^3S_1 ($m = 0$) state to the 2^3P_1 state, thereby driving more than 99% of the metastable atoms in the beam to $m = \pm 1$ state. The atoms then pass through two slits with a width of 1.5 mm and a distance of 700 mm, which constrains the lateral divergence angle of the atomic beam to less than 2.1 mrad. For an atomic beam decelerating to 100 m/s in the longitudinal direction, it is equivalent to selecting atoms with a lateral velocity of <0.21 m/s, which effectively reduces the Doppler broadening effect in precision-spectroscopy measurements. The atoms then hit a 50% duty cycle stainless-steel grid, and the electrons that are generated are detected by a channel multiplier tube as a signal for actively stabilizing the intensity of the beam. After the grid, atoms are excited in the spectral detection zone and pass through a Stern-Gerlach magnetic field with a length of 34 cm. The magnet field has a gradient of about 0.6 T/cm vertical to the atomic beam. Therefore, only metastable helium atoms at the $m = 0$ state can finally reach the detector placed at the end of the beam.

A narrow-linewidth fiber laser is used as the master laser and is locked with a temperature-stabilized Fabry-Pérot cavity made of ultralow-expansion glass. The frequency of the etalon has been measured by using an optical frequency comb, indicating drift of less than 3.6 kHz/hr. A homemade external cavity diode laser near the 1083 nm $2^3S_1 - 2^3P_2$ transition is phase locked with the master laser. After power amplification by a ytterbium-doped fiber amplifier, it is used in 2D-MOTs, beam deflecting, and the Zeeman slower. A distributed feedback laser (DFB) is used as the pump laser

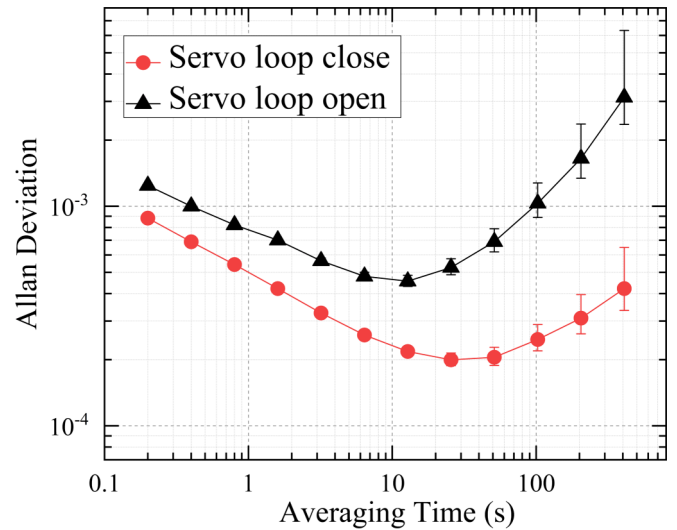


FIG. 2. Relative Allan deviation of atomic-beam stability when the stable beam system is turned on or off.

and its frequency is locked on resonance with the $2^3S_1 - 2^3P_1$ transition. Another narrow-linewidth fiber laser is used for spectral detection whose phase is locked to the positive first-order sideband generated by the master laser through an electro-optic modulator (EOM), allowing the frequency to cover the $2^3S_1 - 2^3P_0$ transition.

Metastable atomic beams prepared by discharge or electronic collision usually have the problem of slow drifting of the number density [27–29], which contributes to statistical uncertainties and eventually limits the experimental accuracy. We use a channel-multiplier tube to sample the triplet metastable helium atomic-beam intensity after Slit2 shown in Fig. 1. A feedback control servo is used to control the frequency of the transverse cooling laser, which effectively stabilizes the beam intensity. In this way, we can adequately compensate for the beam fluctuations in the system due to factors such as instability in discharge, laser power fluctuations, etc. The intensity of the atomic beam that is finally measured is shown in Fig. 2. Black triangles and red circles mark the Allan deviations of the relative fluctuation of the atomic-beam intensity when the proportional integral derivative (PID) feedback loop was open and closed, respectively. When the feedback servo was closed, the relative fluctuation of the atomic-beam intensity after 100 s was reduced by 5–10 times, being as low as 2×10^{-4} . Such high stability considerably reduces the noise in precision spectral measurements.

The method of spectroscopy measurements is similar to that used in our previous experiments [1,23,30,31]. First, a circularly polarized laser is used to evacuate atoms at the $m = 0$ state to obtain a zero background signal. When the spectral probing laser frequency resonates with the transition, due to spontaneous radiation, atoms excited by the probe laser will return to the 2^3S_1 ($m = 0$) state with a certain probability, which can pass through the Stern-Gerlach magnet and be detected, forming a resonance signal. Figure 3 shows the spectrum of the $2^3S_1 - 2^3P_0$ transition obtained by a single scan, and the scan time was about 25 s. The width of the spectrum is about 1.79 MHz (full width at half maximum)

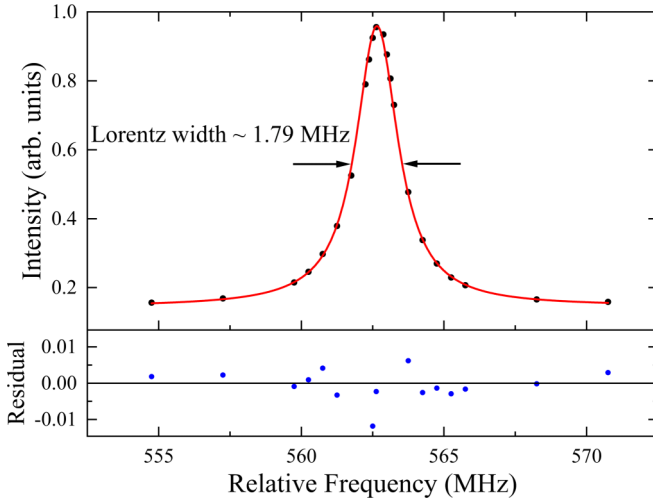


FIG. 3. Experimental (scattering points, single scan) and simulated spectra of the $2^3S_1 - 2^3P_0$ transition. The probe laser power was $0.03 \mu\text{W}$. Fitting residuals are given in the lower panel.

and the corresponding natural line width is 1.62 MHz. The probe laser power was $0.03 \mu\text{W}$ with a diameter of 4 mm, which is only about 1/1000 of the saturated intensity ($167 \mu\text{W cm}^{-2}$). However, a signal-to-noise ratio of over 1000 can be easily achieved in tens of seconds, owing to the excellent stability and high brightness of the atomic beam. Note that at such a low probing laser power, the power-dependent frequency shift [1] could be reduced to well below 1 kHz.

The metastable helium atoms are decelerated by the Zeeman slower with $a = 0.6 a_{\text{max}}$, where $a_{\text{max}} = \hbar k \Gamma / 2m$ is the deceleration due to on-resonance photon scattering, k is the wave vector of the photon, m is the mass of the atom, and Γ is the natural linewidth of the transition. The Zeeman slower has a total length of 115.6 cm and the designed capture range is 100–820 m/s. Taking into account that the atoms have an average speed of 950 m/s at a temperature of 138 K, the capture efficiency is 32.7% for ^4He and 22.0% for ^3He . During the slowing process, the atoms are subjected to random recoil of spontaneous radiation photons, which induce a lateral heating effect [32]. If a parallel Zeeman decelerating laser beam is used, a large number of atoms will escape from the beam, so we used a laser beam that is slightly focused to about 10 mm at the outlet and 5 mm at the inlet of the Zeeman slower. By changing the detuning of the laser frequency and the magnetic field of the slower, the final speed of the helium atoms emitted from the Zeeman slower can be adjusted.

III. RESULTS

As mentioned above, since the Zeeman slower generates transverse heating for the atoms, we use two pairs of anti-Helmholtz coils to form a magneto-optical lens to compress the lateral velocity and focus the metastable helium atom beam [33,34]. At a specific value of the coil working current, atoms of different speeds will focus on different positions. Using a Monte Carlo procedure, we simulated trajectories of atoms with speed around 100 m/s selected by the deflecting laser and two slits, and the results are illustrated in Fig. 4. The

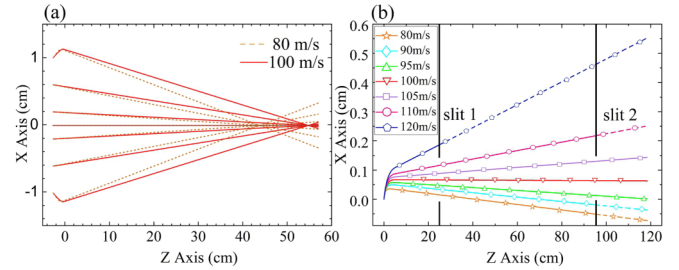


FIG. 4. Simulated trajectories of the atoms in the regions of (a) focusing and (b) deflection. (a) Focusing region: atoms distributed originally in a range of 2 cm with a vertical velocity of 8 m/s and a longitudinal speed of 80 m/s (dashed lines) and 100 m/s (solid lines). (b) Deflection region: atoms with the original longitudinal speed in the range of 80–120 m/s. Two black vertical lines indicate the two slits.

beam propagating direction is chosen as the z axis. The solid and dashed lines in Fig. 4(a) indicate the trajectories of the atoms with an initial v_z of 100 and 80 m/s, respectively. These atoms are spreading in a range of 2 cm and have a maximum vertical velocity v_x of 8 m/s. According to the simulation, atoms with $v_z = 100$ m/s (solid lines) are finally focused near 55 cm downstream from the center of the 2D-MOT, where the deflecting light is located. Atoms with $v_z = 80$ m/s (dashed lines) are focused around 44 cm downstream and have a sizable space distribution along the z axis. When we change the working current of the coil, atoms of different speeds can be selected and focused at the position where the deflecting light is located.

Using the relevant experimental parameters, such as the 5 cm diameter of the deflected laser, the angle between the deflected laser and the beam direction is 80.2° , and the formula of the scattering force of the laser on the atom, we also simulated the flight trajectories of atoms with different velocities when they are deflected by the laser and the results are illustrated in Fig. 4(b). The two solid black lines in the figure indicate two slits, which are both 1.5 mm wide with a distance of 700 mm. The simulation shows that as a result of the combination of the deflected laser and slits, only the atoms with a speed of 100 ± 5 m/s can pass through, which is consistent with the experimental results (see below).

To measure the longitudinal velocity distribution of the atomic beam, we used two probing beams (Fig. 1) to measure the $2^3S_1 - 2^3P_0$ transition of the atoms in the beam. One was perpendicular to the atomic beam, which induced a signal without the first-order Doppler shift. The other one was incident with an angle of 45° . Using the Doppler frequency shift between the signals detected by the two beams, we determined the longitudinal velocity of the atoms.

Figure 5 shows the recorded spectra of beams at different speeds. In each measurement (indicated by one particular symbol), two spectral peaks were observed, representing signals generated by two laser beams of 90° and 45° angle, respectively. All the 90° peaks obtained at different conditions overlap with each other. The laser intensity used in all the measurements was less than 1/50 of the saturated intensity. As a result, the width [full width at half maximum (FWHM)] of the 90° peaks is less than 2 MHz, without noticeable power

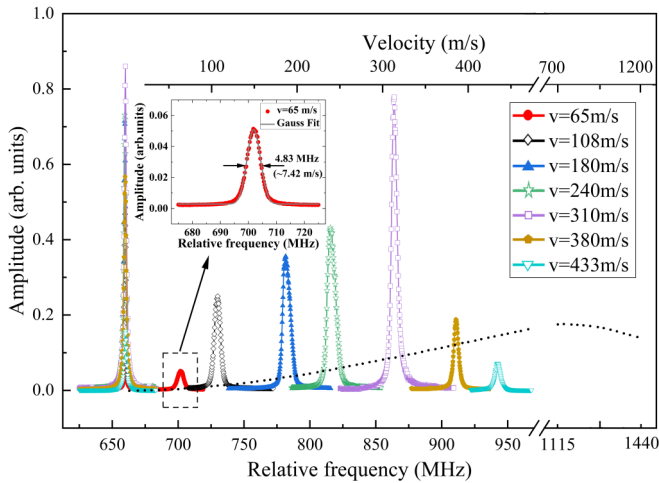


FIG. 5. The $2^3S_1 - 2^3P_0$ spectra recorded under different experimental conditions, where atoms with different speeds were selected. Each symbol and color indicates the spectrum obtained under one condition. Two components correspond to the 45° and 90° probing lasers, respectively. Peaks overlapping at 660 MHz are generated by the 90° probing beam. The black dotted line shows the simulated spectrum of the beam without speed selection, which has a flux of 1.3×10^{14} (atoms/s)/sr and an equilibrium temperature of 138 K. The inset corresponds to the signal with the longitudinal velocity center at 65 m/s, which is relatively weak but still about 40 times that of the thermal equilibrium beam at 138 K (black dotted line).

broadening. The width of the 45° peaks is less than 6 MHz, corresponding to a velocity distribution of less than ± 4.5 m/s. Such a velocity distribution corresponds to an atomic temperature of less than 10 mK. The experimental result is consistent with our simulation. Only atoms with a very narrow velocity distribution can pass through the deflecting region and the two slits downstream. For comparison, we also simulated the spectrum of the beam without speed selection, which has a flux of 1.3×10^{14} (atoms/s)/sr and an equilibrium temperature of 138 K. The simulated spectrum has a very broad feature and the result is also shown as the black dotted line in Fig. 5. The figure shows that the longitudinal speed of the atomic beam can be adjusted from 50 to 450 m/s, being close to a span of an order of magnitude, and the accuracy is better than 2%. The inset of Fig. 5 illustrates the spectrum of atoms with a speed of 65 m/s, showing a signal-to-noise ratio of over 200. Moreover, the amplitude is about 40 times that of a thermal equilibrium beam at 138 K with a total flux of 1.3×10^{14} (atoms/s)/sr.

It can be seen that the amplitudes of the signal, which correspond to the intensity of the atomic beam, vary considerably at different selected speeds. The reason is as follows. When fast atoms are selected, large laser power is needed to deflect the atoms, which brings an additional heating effect and increases the transverse velocity of the atoms. Consequently,

many atoms are lost during passing through the narrow slit. When slow atoms are selected, it takes a longer time for the atoms to pass through the Zeeman slower and the slits, which also induces loss of atoms due to the transverse divergence of the beam. Therefore, when a particular longitudinal speed is selected, we need to refine the experimental conditions, which lead to different deceleration and deflection efficiency. At the velocity of 310 ± 4.5 m/s, the flow rate of the metastable atoms was 3×10^7 atoms/s, measured by a calibrated channel multiplier tube at a distance of 7 m from the beam source. It is about 30 times greater than that obtained in our previous study [23]. Taking into account the geometrical configuration of the two slits and the aperture (~ 10 mm) of the Stern-Gerlach magnets, we estimate that the active area of the detector is about 0.8 cm^2 . The flux of the metastable helium atoms can be calculated to be 1.8×10^{13} (atoms/s)/sr at this speed.

IV. CONCLUSION

In conclusion, we built a continuous beam of helium atoms populated on the single-quantum state of 2^3S_1 , with high brightness and narrow speed distribution. The adjustable range of the longitudinal speed of the atomic beam is 50–450 m/s, with a half width of less than 4.5 m/s, equivalent to a translation temperature of 10 mK. The flux of the atoms at a single speed has been maintained to be 1.8×10^{13} (atoms/s)/sr, with a fractional fluctuation of 0.02% in a period of 100 s. This device allows considerable improvement in the precision spectroscopy of the helium atom. First, the power shift could be reduced by using a relatively low-power probing laser since the beam flux has been improved by an order of magnitude from that used in previous studies [1,23,30,31]. Second, the decelerated atoms also reduce the first-order Doppler shift in the case of nonorthogonal crossing between the probe laser and the beam. Moreover, by changing the velocity of the atoms, the systematic uncertainty in the measurement could be investigated. With that, we expect to explain the reasons for the recent deviations among the results from beam-based laser-spectroscopy measurements and other methods [35–37], which will eventually lead to a more accurate determination of the helium nuclear charge radius. Atomic beams with a precisely adjustable speed can also be used to change the relative speed parameters, which are critical in collision experiments of neutral atoms and molecules.

ACKNOWLEDGMENTS

This work is jointly supported by the Natural Science Foundation of China (Grants No. 91736101, No. 21688102, No. 11304303, No. 91436209, and No. 21427804), by the Chinese Academy of Science (Grants No. XDB21010400 and No. XDB21020100), and by the Anhui Initiative in Quantum Information Technologies (Grant No. AHY110000).

[1] X. Zheng, Y. R. Sun, J.-J. Chen, W. Jiang, K. Pachucki, and S.-M. Hu, *Phys. Rev. Lett.* **119**, 263002 (2017).

[2] A. Beyer, L. Maisenbacher, A. Matveev, R. Pohl, K. Khabarova, A. Grinin, T. Lamour, D. C. Yost, T. W. Hänsch, N. Kolachevsky, and T. Udem, *Science* **358**, 79 (2017).

- [3] R. Wynands and S. Weyers, *Metrologia* **42**, S64 (2005).
- [4] K. B. Davis, M. O. Mewes, M. R. Andrews, N. J. van Druten, D. S. Durfee, D. M. Kurn, and W. Ketterle, *Phys. Rev. Lett.* **75**, 3969 (1995).
- [5] I. Bloch, T. W. Hänsch, and T. Esslinger, *Phys. Rev. Lett.* **82**, 3008 (1999).
- [6] E. Vliegen, H. J. Wörner, T. P. Softley, and F. Merkt, *Phys. Rev. Lett.* **92**, 033005 (2004).
- [7] B. C. Sawyer, B. K. Stuhl, D. Wang, M. Yeo, and J. Ye, *Phys. Rev. Lett.* **101**, 203203 (2008).
- [8] M. Kirste, L. Scharfenberg, J. Klos, F. Lique, M. H. Alexander, G. Meijer, and S. Y. T. van de Meerakker, *Phys. Rev. A* **82**, 042717 (2010).
- [9] R. Krems, *Phys. Chem. Chem. Phys.* **10**, 4079 (2008).
- [10] V. Zhelyazkova, M. Žeško, H. Schmutz, J. A. Agner, and F. Merkt, *Mol. Phys.* **117**, 2980 (2019).
- [11] P. Jansen, L. Semeria, L. E. Hofer, S. Scheidegger, J. A. Agner, H. Schmutz, and F. Merkt, *Phys. Rev. Lett.* **115**, 133202 (2015).
- [12] L. Semeria, P. Jansen, G. Clausen, J. A. Agner, H. Schmutz, and F. Merkt, *Phys. Rev. A* **98**, 062518 (2018).
- [13] C. G. Parthey, A. Matveev, J. Alnis, B. Bernhardt, A. Beyer, R. Holzwarth, A. Maistrou, R. Pohl, K. Predehl, T. Udem, T. Wilken, N. Kolachevsky, M. Abgrall, D. Rovera, C. Salomon, P. Laurent, and T. W. Hänsch, *Phys. Rev. Lett.* **107**, 203001 (2011).
- [14] K. Pachucki and V. A. Yerokhin, *Phys. Rev. Lett.* **104**, 070403 (2010).
- [15] K. Pachucki and V. A. Yerokhin, *Can. J. Phys.* **89**, 95 (2011).
- [16] G. W. Drake, *Can. J. Phys.* **80**, 1195 (2002).
- [17] K. Pachucki, *Phys. Rev. Lett.* **97**, 013002 (2006).
- [18] K. Pachucki and V. A. Yerokhin, *Phys. Rev. A* **79**, 062516 (2009).
- [19] K. Pachucki and V. A. Yerokhin, *J. Phys.: Conf. Ser.* **264**, 012007 (2011).
- [20] V. Patkóš, V. A. Yerokhin, and K. Pachucki, *Phys. Rev. A* **94**, 052508 (2016).
- [21] N. Bezginov, T. Valdez, M. Horbatsch, A. Marsman, A. C. Vutha, and E. A. Hessels, *Science* **365**, 1007 (2019).
- [22] R. Pohl, A. Antognini, F. Nez, F. D. Amaro, F. Biraben, J. M. R. Cardoso, D. S. Covita, A. Dax, S. Dhawan, L. M. P. Fernandes, A. Giesen, T. Graf, T. W. Hänsch, P. Indelicato, L. Julien, C.-Y. Kao, P. Knowles, E.-O. Le Bigot, Y.-W. Liu, J. A. M. Lopes, L. Ludhova, C. M. B. Monteiro, F. Mulhauser, T. Nebel, P. Rabinowitz, J. M. F. dos Santos, L. A. Schaller, K. Schuhmann, C. Schwob, D. Taqqu, J. F. C. A. Veloso, and F. Kottmann, *Nature (London)* **466**, 213 (2010).
- [23] X. Zheng, Y. R. Sun, J.-J. Chen, W. Jiang, K. Pachucki, and S.-M. Hu, *Phys. Rev. Lett.* **118**, 063001 (2017).
- [24] N. Vansteenkiste, C. Gerz, R. Kaiser, L. Hollberg, C. Salomon, and A. Aspect, *J. Phys. II* **1**, 1407 (1991).
- [25] W. Rooijakkers, W. Hogervorst, and W. Vassen, *Opt. Commun.* **123**, 321 (1996).
- [26] Y. R. Sun, G.-P. Feng, C.-F. Cheng, L.-Y. Tu, H. Pan, G.-M. Yang, and S.-M. Hu, *Acta Phys. Sin.* **61**, 170601 (2012).
- [27] D. Fahey, W. Parks, and L. Scheerer, *J. Phys. E: Sci. Instrum.* **13**, 381 (1980).
- [28] E. W. Rothe, R. H. Neynaber, and S. M. Trujillo, *J. Chem. Phys.* **42**, 3310 (1965).
- [29] C.-F. Cheng, W. Jiang, G.-M. Yang, Y.-R. Sun, H. Pan, Y. Gao, A.-W. Liu, and S.-M. Hu, *Rev. Sci. Instrum.* **81**, 123106 (2010).
- [30] G.-P. Feng, X. Zheng, Y. R. Sun, and S.-M. Hu, *Phys. Rev. A* **91**, 030502(R) (2015).
- [31] X. Zheng, Y. R. Sun, J.-J. Chen, J.-L. Wen, and S.-M. Hu, *Phys. Rev. A* **99**, 032506 (2019).
- [32] W. Rooijakkers, W. Hogervorst, and W. Vassen, *Opt. Commun.* **135**, 149 (1997).
- [33] G. Labeyrie, A. Browaeys, W. Rooijakkers, D. Voelker, J. Groperrin, B. Wanner, C. I. Westbrook, and A. Aspect, *Eur. Phys. J. D* **7**, 341 (1999).
- [34] M. Hoogerland, J. Driessen, E. Vredenburg, H. Megens, M. Schuwer, H. Beijerinck, and K. Van Leeuwen, *Appl. Phys. B* **62**, 323 (1996).
- [35] P. C. Pastor, G. Giusfredi, P. De Natale, G. Hagel, C. de Mauro, and M. Inguscio, *Phys. Rev. Lett.* **92**, 023001 (2004).
- [36] P. C. Pastor, G. Giusfredi, P. De Natale, G. Hagel, C. de Mauro, and M. Inguscio, *Phys. Rev. Lett.* **97**, 139903(E) (2006).
- [37] P. C. Pastor, L. Consolino, G. Giusfredi, P. De Natale, M. Inguscio, V. A. Yerokhin, and K. Pachucki, *Phys. Rev. Lett.* **108**, 143001 (2012).